Neurophysiol. **46**, 755 (1981).
4. E. De Renzi, *Disorders of Space Exploration* (Wiley, New York, 1982); M. M. Mesulam, *Ann. Neurol.* **10**, 309 (1981); M. I. Posner, J. A. Walker, F. J. Friedrich, R. D. Rafal, *J. Neurosci.* **4**, 1863 (1984).
5. M. Corbetta, F. M. Miezin, G. L. Shulman, S. E. Petersen, *J. Neurosci.* **13**, 1202 (1993).
6. In a psychophysical session before the PET session, participants' reaction times for the color and motion tasks were equated, and participants practiced the conjunction task. During the color blocks, the similarity of the target and distractor colors was varied. The distractor color that yielded reaction times most similar to the reaction times in the motion task was chosen for the following PET session.
7. During the PET session, each task was presented twice, with target probabilities of 0.2 and 0.8 in different blocks. These changes in probability were introduced to study the neural systems involved in target detection, but they are not part of this report. PET scans were performed with a PET VI scanning system [M. Yamamoto, D. C. Ficke, M. M. Ter-Pergossian, *IEEE Trans. Nucl. Sci.* **29**, 529 (1982)] and the standard ^{15}O-labeled (half-life, 123 s) water bolus injection technique, which has been previously described [P. Herscovitch, J. Markham, M. E. Raichle, *J. Nucl. Med.* **24**, 782 (1983)]. Scans were 40 s long, which allowed nine scans to be acquired during a single session. Images were obtained from each participant for each experimental condition and were normalized to a common value. For each participant, change images corresponding to specific conditions (see text) were created by subtraction of one image from another. All change images were transformed to a standard stereotactic space [J. Talairach and P. Tournoux, *Co-Planar Stereotaxic Atlas of the Human Brain* (Georg Thieme Verlag, Stuttgart, Germany, 1988); P. T. Fox, J. Perlmutter, M. E. Raichle, *J. Comput. Assisted Tomogr.* **9**, 141 (1985)] and then averaged across participants. The averaged subtraction image was then searched to identify the magnitude and location in stereotactic coordinates of all positive and negative local maxima [P. T. Fox, M. A. Mintun, E. M. Reiman, M. E. Raichle, *J. Cereb. Blood Flow Metab.* **8**, 642 (1988); M. A. Mintun, P. T. Fox, M. E. Raichle, *ibid.* **9**, 96 (1989)].
8. Participants were always instructed to maintain fixation, which was monitored by means of electrooculography. The fixation scan was presented in position 5, and the two passive scans were presented in positions 3 and 7. The color and motion scans were counterbalanced over positions 1, 2, 4, and 6, whereas the two conjunction scans occurred in positions 8 and 9. Although the conjunction conditions were presented after the color and motion conditions, it is unlikely that differences between conditions were caused by this factor. We did not observe any effect of this nature in a similar experiment [D. L. Hunton, M. Corbetta, G. L. Shulman, F. M. Miezin, S. E. Petersen, in preparation] in which task order was balanced. Moreover, there was no difference between the early (scan 3) and late (scan 7) passive conditions.
9. Participants performed three blocks of 66 trials for each task, and target probability was fixed at 0.5.
10. A 2:1 ratio of slopes in the target-absent and target-present conditions is sometimes considered a diagnostic for serial self-terminating search. In the present experiment, the slope in the target-absent condition (9 ms per item) of the conjunction task was actually less than that for the target-present condition (25 ms per item). The relative ease of the target-absent condition may reflect the use of a single distractor value rather than multiple distractor values (*1*). There also appears to have been a criterion shift toward no-target responses, perhaps because of the fixed display duration, with a significant main effect of response [$F(1,14) = 14.9$; $P < 0.005$] in the error data.
11. The activations during the conjunction task for both the left and right superior parietal regions were consistent when either the passive or fixation-point control was used. During the feature tasks, participants showed no activity in the right parietal region when either control condition was used. The left parietal activity during the feature tasks was more variable, with more color-related activity in the fixation-point control and more motion-related activity in the passive control, as reported in Table 1.
12. Participants' reaction time to targets occurring at predicted locations was significantly faster than their reaction time to targets occurring at nonpredicted locations. This advantage in reaction times is typically interpreted as reflecting shifts of attention to the predicted location. Because no stimulation occurred at the predicted location before the shift of attention, these shifts were driven endogenously, as in the conjunction task.
13. Quantitatively, all superior parietal activations with a magnitude greater than 20 counts were selected from the shifting-attention image. This magnitude is based on an estimation of significant responses for different sample sizes. This procedure yielded coordinates from two right hemispheric foci and one left hemispheric focus, which were applied to the present data set. For each participant, a sphere with a radius of 7 mm, based on the spatial resolution of the scanner, was centered on each focus. This sphere was applied separately to the conjunction, color, and motion images, with the passive as control, and the magnitude of activation at each locus was determined. This replication analysis is an unbiased way to test hypotheses about patterns of activation at prespecified brain locations and provides reliable estimates of local probability [see R. L. Buckner *et al.*, *J. Neurosci.* **15**, 12 (1995) for a more complete description of method and rationale].
14. Initially, an ANOVA with task and target probabilities was conducted. Because this analysis yielded no main effect or interaction involving target probability, this factor was collapsed in the one-factor ANOVAs presented in the text. We obtained similar results using all available information in a between-participants design, in which data from some scan pairs for some participants were eliminated due to movement artifacts. A similar feature-conjunction asymmetry at the same right parietal region has been replicated in a recent experiment involving color and orientation perception (*8*).
15. M. Corbetta, F. M. Miezin, S. Dobmeyer, G. L. Shulman, S. E. Petersen, *J. Neurosci.* **8**, 2383 (1991).
16. H. J. Heinze *et al.*, *Nature* **372**, 543 (1995).
17. We thank the reviewers for their helpful suggestions. Supported by NIH grants NS06833, NS2533, and EY08775; ONR grant N00014-89-J-1426; and the McDonnell Center for the Study of Higher Brain Function.

26 April 1995; accepted 4 August 1995

Positional Cloning and Sequence Analysis of the *Drosophila* Clock Gene, *timeless*

Michael P. Myers, Karen Wager-Smith, Cedric S. Wesley, Michael W. Young,* Amita Sehgal

The *Drosophila* genes *timeless* (*tim*) and *period* (*per*) interact, and both are required for production of circadian rhythms. Here the positional cloning and sequencing of *tim* are reported. The *tim* gene encodes a previously uncharacterized protein of 1389 amino acids, and possibly another protein of 1122 amino acids. The arrhythmic mutation tim^{01} is a 64–base pair deletion that truncates TIM to 749 amino acids. Absence of sequence similarity to the PER dimerization motif (PAS) indicates that direct interaction between PER and TIM would require a heterotypic protein association.

Circadian behavioral rhythms, such as human sleep-wake and insect locomotor activity cycles, persist in constant environmental conditions with a period of about a day. Although the phases of such rhythms can be reset by environmental stimuli, particularly light, propagation of the rhythms in the absence of environmental cues indicates action of an endogenous physiological process. Genetic studies of circadian rhythmicity began in earnest with the discovery of clock mutants in *D. melanogaster* (*1*). The mutations affected an X chromosome–linked gene, *per* (*1*, *2*). Recent work has shown that in wild-type flies *per* is expressed with a circadian rhythm, in which peak levels of *per* mRNA are observed near the end of the day (*3*, *4*). *per* mutations that abolish or alter the period length of behavioral rhythms produce parallel effects on the *per* transcript rhythm (*3*, *4*). The PER protein is predominantly nuclear (*5*–*7*) and also accumulates with a circadian rhythm (*5*, *6*, *8*, *9*). However, PER is most abundant late at night when *per* RNA levels are low (*5*, *8*, *9*, *10*). These observations, and the finding that constitutive overexpression of PER protein can substantially diminish the *per* mRNA rhythm in certain cells of the fly (*10*), are consistent with the proposal that PER negatively regulates expression of its own mRNA (*3*). Such feedback control may be indirect, because PER lacks a known DNA binding motif (*11*).

PER contains a sequence with homology to a domain (PAS) found in three basic helix-loop-helix (bHLH) transcription factors (*12*, *13*). The PAS domain of PER can support dimerization, or alternatively, intramolecular binding to a nonhomologous sequence located on the COOH-terminal side of the PAS domain (*14*, *15*). Two proteins containing PAS, AHR and ARNT, also interact to form the activated aryl hydrocarbon receptor (*13*, *16*). These

M. P. Myers, K. Wager-Smith, C. S. Wesley, M. W. Young, Howard Hughes Medical Institute, National Science Foundation Science and Technology Center for Biological Timing, and Laboratory of Genetics, Rockefeller University, New York, NY 10021, USA.
A. Sehgal, Department of Neuroscience and Center for Sleep and Respiratory Neurobiology, University of Pennsylvania School of Medicine, Philadelphia, PA 19104, USA.
*To whom correspondence should be addressed.

findings suggest that PER might associate with an unknown partner or partners through its PAS domain.

The chromosome 2–linked *timeless* (*tim*) mutation produces phenotypes analogous to those of the mutation per^0: rhythmic eclosion, locomotor activity, and rhythmic expression of *per* mRNA are abolished (*4*). The latter observation indicates that the *per* and *tim* genes interact at some level. Additional evidence for such an interaction shows that tim^+ activity is necessary for nuclear localization of a PER–β-galactosidase (PER–β-Gal) fusion protein expressed in transgenic flies (*9*). PER–β-Gal fusion proteins were readily detected in the cytoplasm of *tim* flies, but endogenous PER was not, which suggests that PER may be stabilized by transport to the nucleus in wild-type flies (*9*). The PAS domain may control PER subcellular localization, because a PER fusion protein without a PAS-containing region was constitutively nuclear, even in *tim* flies (*9*). Protein immunoblot analyses of extracts from *tim* flies show that PER levels are very low and do not oscillate (*17*). As a result of these effects of the *tim* mutation on *per* mRNA and protein, it was proposed that a central aspect of the *Drosophila* clock might entail time-dependent nuclear localization of PER regulated by the product of *tim* (*9*).

The *tim* mutation was mapped to an interval between *dpp* and *dp* that corresponds to approximately 2 to 3 megabase pairs (Mbp) of DNA (*4*). Further recombination mapping localized *tim* to a region bounded by *male-sex lethal 2* (*msl-2*) and *odd-skipped* (*odd*) (Fig. 1). A chromosome deficiency with breakpoints in polytene bands 23D and 23F [$Df(2L)DTD62\ 2^P\ 3^D$; $H7\ 3^P\ 2^D$ (*18*)] genetically complemented the *tim* mutation and placed *tim* proximal to the deficiency breakpoint in 23F (Fig. 1A). This deficiency did not complement *msl-2* (Fig. 1A), which made its breakpoint in 23F the nearest marker on the distal side of *tim*. We characterized a new deficiency chromosome that fails to complement the *tim* mutation, and have designated it $Df(2L)tim^{02}$ (Fig. 1A) (*19*). Accordingly, we have renamed the original *tim* mutation tim^{01}. Cytological analysis of polytene chromosomes from $Df(2L)tim^{02}$ revealed loss of a portion of 23F (23F3-6) and possibly diminution of 24A1 (*19*). $Df(2L)DTD62\ 2^P\ 3^D$; $H7\ 3^P\ 2^D$ and $Df(2L)tim^{02}$ are each homozygous lethal, and genetic crosses between them failed to yield viable trans-heterozygotes, indicating that they overlap and disrupt at least one common essential gene. A set of three homozygous lethal deficiencies that remove *Abnormal leg pattern* [*Df(2L) Alp77*, *Df(2L) Alp101*, and *Df(2L) Alp177* (*20*)] complement tim^{01} and $Df(2L)tim^{02}$, further reducing the interval containing *tim* because *Alp* is distal to *odd* (Fig. 1A).

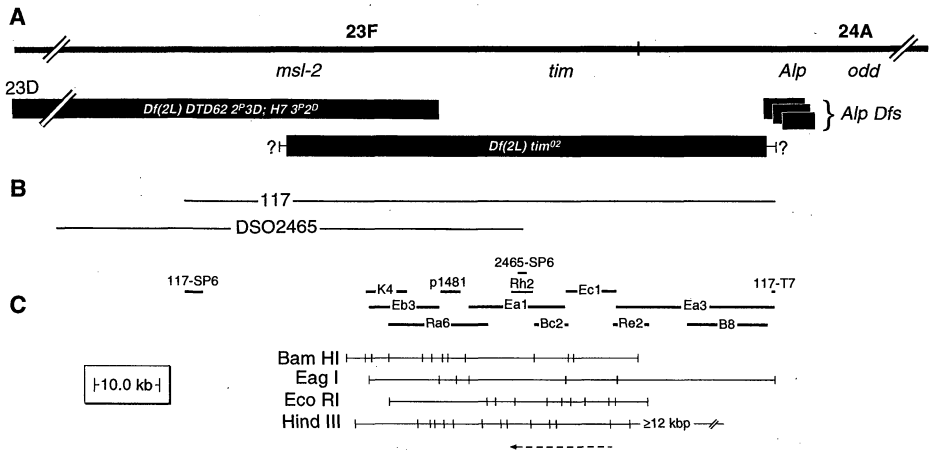

Fig. 1. Schematic of *tim* locus on chromosome 2. The corresponding regions in (A) to (C) are in vertical register. (**A**) Mapping of *tim* by complementation tests with chromosome deficiencies. The deficiencies are depicted as solid bars representing the genetic material missing from the chromosome. Although $Df(2L)DTD62\ 2^P\ 3^D$; $H7\ 3^P\ 2^D$ is a synthetic deletion composed of two nonoverlapping translocations of chromosome 2 to 3 (*18*), for simplicity it is shown as a continuous deletion of chromosome 2. The proximal breakpoint of $Df(2L)DTD62\ 2^P\ 3^D$; $H7\ 3^P\ 2^D$ is located within clone Ra6 (C). The distal breakpoint of $Df(2L)tim^{02}$ lies to the left of *msl-2*, but has not been mapped further. The proximal breakpoint of $Df(2L)tim^{02}$ maps proximal to clone Ea3 and distal to a vital gene uncovered by the *Alp* deficiencies. (**B**) Overlapping P1 clones 117 (*21*), and DSO2465 used to generate a contig covering *tim*. (**C**) DNA clones and PCR products from the *tim* contig are shown in bold lines, and the restriction maps for Bam HI, Eag I, Eco RI, and Hind III corresponding to this region are shown. Clones K4 and p1481 were isolated by plasmid rescue from the P stocks 101-1 and P1481, respectively. P1481 and two other P-element insertions located within 200 bp (145-7, 145-12) were all found to be unlinked to the lethal phenotype on which they were originally isolated (*24*). Clone B8 is from a chromosome walk covering the *Alp* gene (*20*).

To correlate the genetic and cytological maps with a physical map consisting of cloned DNA, we obtained P1-based genomic DNA clones and P-element insertion stocks that mapped to the region 23F-24A. Additional clones were from a chromosomal walk covering *msl-2* (*21*). End-specific DNA probes from the P1 and cosmid inserts were obtained by polymerase chain reaction (PCR) (*22*), and DNA flanking each P-element insertion was cloned by plasmid rescue (*23*). These probes were used in DNA blot analyses to produce a restriction map of the region and subclone an overlapping set of Eag I, Eco RI, and Bam HI fragments from the P1 clone 117, yielding a 60-kb contig (Fig. 1, B and C).

The proximal breakpoint in $Df(2L)DTD62\ 2^P\ 3^D$; $H7\ 3^P\ 2^D$ was mapped to the Eco RI fragment Ra6 by DNA blot analysis (*24*), thereby providing a physical anchor for the distal border of the interval containing *timeless* (Fig. 1C). DNA blot analysis also revealed that DNA from the entire 60-kb contig is absent in $Df(2L)tim^{02}$, consistent with the genetic complementation tests. A DNA clone (B8) from a chromosomal walk covering *Alp* (*20*) overlaps with our contig (Fig. 1C), indicating that the proximal breakpoint in $Df(2L)tim^{02}$ must lie very near to the end of the contig yet leaves the *Alp* gene intact.

Because tim^{01} was produced by a hybrid dysgenesis screen (*4*) rather than by chemical mutagenesis, we reasoned that the causative lesion might involve a deletion or insertion of DNA that could be detected as a restriction fragment length polymorphism (RFLP). Indeed, a DNA blot comparison of DNA from tim^{01} and its wild-type parental line (R702.1TP) with the subclone Ec1 as probe detected RFLPs for the enzymes Eco RI and Hinf I. One of four Eco RI fragments detected by Ec1, a 2.2-kb fragment in the parental line, was reduced in size in DNA from tim^{01} flies (Fig. 2A). The remaining Eco RI fragments displayed no change in size, signifying the presence of a small deletion within the 2.2-kb fragment in tim^{01} flies. Two additional tim^{01} sublines, established and separately maintained from the time of the mutant's initial recovery (*4*), also showed evidence of this deletion upon DNA blot analysis (*24*). This result indicated that the deletion arose in conjunction with the mutant phenotype. The Ec1 probe also detected a reduction in the size of one of several Hinf I fragments derived from tim^{01} DNA. The change was estimated to be a deletion of about 70 bp (Fig. 2B). None of the other subclones in the contig detected RFLPs between DNA from tim^{01} and R702.1TP for the enzymes Eco RI, Bam HI, Hind III, Hinf I, Alu I, Fok I, Hae III, Rsa I, or Taq I (*24*). The location of the deletion in tim^{01} flies also agrees well with the position of the mutation predicted from

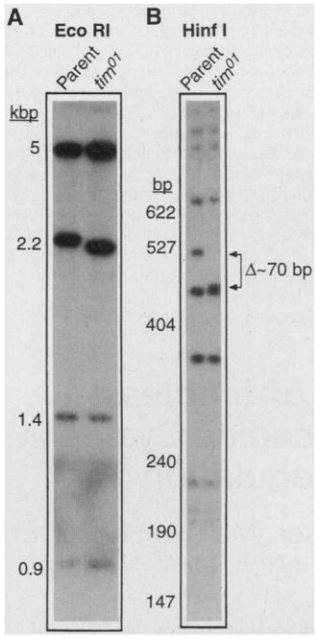

Fig. 2. Restriction fragment length polymorphisms (RFLPs) detected in *tim*^{01}. DNA blots were prepared containing DNA from *tim*^{01} and the wild-type parental flies, after digestion with Eco RI (**A**) or Hinf I (**B**), and probed with the genomic DNA clone Ec1 (Fig. 1C). The gel in (A) was standard 1% agarose and in (B) was 2% MetaPhor Agarose (FMC Bioproducts, Rockland, Maine).

```
1    MSRVRQLHNH IWNNQNFDKV KSVMDWLLAT PQLYSAFSSL GCLEGDTYVV
51   NPNALAILEE INYKLTYEDQ TLRTFRRAIG FGQNVRSDLI PLLENAKDDA
101  VLESVIRILV NLTVPVECLF SVDVMYRTDV GRHTIFELNK LLYTSKEAFT
151  EARSTKSVVE YMKHILESDP KLSPHKCDQI NNCLLLLRNI LHIPETHAHC
201  VMPMMQSMPH GISMQNTILW NLFIQSIDKL LLYLMTCPQR AFWGVTMVQL
251  IALIYKDQHG SGDSSPMLTS DPTSDSSDNG SNGRGMGGGM REGTAATLQE
301  VSRKGQEYQN AMARVPADKP DGSEEASDMT GNDSEQPGSP EQSQPAGESM
351  [redacted] YLQLGPASEP LNLTQQPADK
401  VNNTTNPTSS APQGCLGNEP FKPPPPLPVR ASTSAHAQMQ KFNESSYASH
451  VSAVKLGQKS PHAGQLQLTK GKCCPQKREC PSSQSELSDC GYGTQVENQE
501  SISTSSNDDD GPQGKPQHQK PPCNTKPRNK PRTIMSPMD [redacted]
551  [redacted]SSLINMK GLVQHTPTDD DISNLLKEFT VDFLLKGYSY LVEELHMQLL
601  SNAKVPIDTS HFFWLVTYFL KFAAQLELDM EHIDTILTYD VLSYLTYEGV
651  SLCEQLELNA RQEGSDLKPY LRRMHLVVTA IREFLQAIDT YNKVTHLNED
701  DKAHLRQLQL EISEMSDLRC LFVLLLRRFN PSIHSKQYLQ DLVVTNHILL
751  LILDSSAKLG GCQTIRLSEH ITQFATLEVM HYYGILLEDF NNNGEFVNDC
801  IFTMMHHIGG DLGQIGVLFQ PIILKTYSRI WEADYELCDD WSDLIEYVIH
851  KFMNTPPKSP LTIPTTSLTE MTKEHNQEHT VCSWSQEEMD TLYWYYVQSK
901  KNNDIVGKIV KLFSNNGNKL KTRISIIQQL LQQDIITLLE YDDLMKFEDA
951  EYQRTLLTTP TSATTESGIE IKECAYGKPS DDVQILLDLI IKENKAQHLL
1001 WLQRILIECC FVKLTLRSGL KVPEGDHIME FVAYHCICKQ KSIPVVQWNN
1051 EQSTTMLYQP FVLLLHKLGI QLPADAGSIF ARIPDYWTPE TMYGLAKKLG
1101 PLDKLNLKFD ASELEDATAS SPSRYHHTGP RNSLSSVSSL DVDLGDTEEL
1151 ALIPEVDAAV EKAHAMASTP SPSEIFAVPK TKHCNSIIRY TPDPTPPVPN
1201 WLQLVMRSKC NHRTGPSGDP SDCVGSSSTT VDDEGFGKSI SAATSQAAST
1251 SMSTVNPTTT LSLNMLNTFM GSHNENSSSS GCGGTVSSLS MVALMSTGAA
1301 GGGGNTSGLE MDVDASMKSS FERLEVNGSH FSRANNLDQE YSAMVASVYE
1351 KEKELNSDNV SLASDLTRMY VSDEDDRLER TEIRVPHYH
```

Fig. 3. Conceptual translation of *tim*. The sequence shown corresponds to the 1389–amino acid open reading frame generated when the retained intron is spliced out. The black arrowhead marks the position of the deletion in *tim*^{01}. After residue 714, the new reading frame terminates with the sequence ISIFRIWWLPITSSYSFWTVRPNLVDVKPFACRST. The unfilled arrowhead marks the position of the alternative COOH-terminal sequence generated by the retained intron. Residue 1105 is converted from L to R, followed by the sequence ELKST TEKNNPFVIPQR. The acidic domain and potential NLS are indicated as white text on black. Single-letter abbreviations for the amino acid residues are as follows: A, Ala; C, Cys; D, Asp; E, Glu; F, Phe; G, Gly; H, His; I, Ile; K, Lys; L, Leu; M, Met; N, Asn; P, Pro; Q, Gln; R, Arg; S, Ser; T, Thr; V, Val; W, Trp; and Y, Tyr. The *tim* DNA sequence has been deposited with GenBank (accession number U37018).

genetic recombination studies. *tim*^{01} was located ~0.16 map units (2 recombinants/1248 tested chromosomes) proximal to *msl-2*, which should correspond to a physical distance of ~40 to 50 kb (*25*). Together, these results strongly indicated that the identified deletion produces the *tim* mutant phenotype. Further evidence has been derived from sequencing the mutant DNA (below) and from our finding that this gene is expressed with a circadian rhythm that is altered in *per* and *tim* mutants (*26*), and produces a protein that directly and specifically binds PER (*27*).

We used Ec1 to screen a head-specific complementary DNA (cDNA) library (*28*). Several positive recombinant phage were purified, converted to plasmid clones, and the inserts restriction mapped. Clone 35c (*24*) extended the farthest in the 5′ direction. The remaining cDNAs, 35a, d, e, g and 22g (*24*), although incomplete at their 5′ ends, have identical 3′ ends and contain a consensus polyadenylation signal. Combining the partial cDNAs at their sites of overlap yields a complete cDNA of 5192 bp. Sequencing all of 35c and significant portions of the other clones revealed an open reading frame coding for 1122 amino acids (Fig. 3). To guard against possible artifacts in the cDNA library, we also sequenced genomic DNA (clones Ec1 and Ea1) to confirm the exon content (*24*). One of the cDNA clones, 22g, showed a deletion of 237 bp relative to the other cDNAs. The sequence missing from 22g corresponds to an intron retained in the other clones, with consensus 5′ and 3′ splice signals. Its removal in 22g extends the open reading frame to 1389 amino acids (Fig. 3), yielding a protein with a predicted molecular mass of 156 kD. Complementary DNAs encoding the longer form of TIM protein (that is, lacking the 237-bp intron) were also obtained from an independently constructed head cDNA library as described in our companion report (*27*). Therefore, because of a retained intron in certain transcripts, there may be two forms of the TIM protein; each would share residues 1 to 1104 but have different COOH-termini. Retained introns with varying degrees of coding potential have been observed for several genes (*29*). Given the likelihood that each form of TIM protein would have distinct activities, experiments to confirm the presence of the intron-bearing *tim* transcripts are in progress. At a minimum, we expect the 1389-residue form of TIM to be expressed and to function in the adult fly head.

In order to characterize the deletion detected in *tim*^{01}, we used PCR to amplify and sequence DNA corresponding to the 2.2 kb Eco RI fragment from the parental line (R702.1TP) and *tim*^{01}. A 64-bp deletion was detected in the *tim*^{01} DNA, very close to the size estimated from the Hinf I RFLP. The deletion causes a frame shift in the sequence encoding TIM, and the predicted translation product contains amino acids 1 to 714, with an additional 35 residues from the new reading frame (Fig. 3). We confirmed the 64-bp deletion as the sole change in *tim*^{01} that affects the translated product by sequencing all exons 5′ of the deletion (*30*). Thus, if stably expressed, the TIM protein in *tim*^{01} flies is only about half its normal length and probably lacks activity. Moreover, because the phenotypes of *tim*^{01}/*tim*^{01} and *tim*^{01}/*Df(2L)tim*^{02} flies are indistinguishable, we regard *tim*^{01} as a null mutation.

Database comparisons with either form of TIM yielded no significant homologies. Analysis of the amino acid sequence showed no evidence of a signal sequence in the NH_2-terminus; thus, TIM is not likely to be a secreted protein or a cell surface receptor. The TIM sequence contains a basic region (KKELRRKKLVKRSK) that could potentially function as a nuclear localization signal (NLS). It also contains an extensive acidic region (DDGDYEDQRHRQLNEHGEEDEDEDEVEEEE), a characteristic feature of the activation domain in some transcription factors. TIM is quite acidic overall, with a calculated isoelectric point of 5.14.

We were surprised to find an absence of sequence homology between PER and TIM, as our accompanying report demonstrates a physical interaction between these two proteins that is mediated by the PAS domain in PER (*27*). Earlier studies indicated that PAS-containing proteins, including PER, can dimerize or associate with each other through homotypic interactions of their PAS domains (*14, 31*). Nevertheless, careful inspection of the predicted TIM sequence in this study failed to indicate a region of homology to PAS. A heterotypic intramolecular interaction of PAS with a distinct region of PER (the C-domain, residues 524 to 685) has been reported (*15*), but TIM shares no sequence similarity to this region either. Thus, with at least three

different protein targets, the PAS domain in PER exhibits great flexibility in mediating protein-protein interactions. This may have implications regarding the number of potential interacting targets for other PAS-containing proteins.

Molecular cloning of *tim* has allowed the detection of circadian cycles in *tim* RNA expression (26). Our combined molecular studies reveal a tight interplay between PER and TIM and suggest a rudimentary intracellular biochemical mechanism regulating circadian rhythms in *Drosophila*. Further analysis of *tim* and its interactions with *per* will likely shed new light on this central clock mechanism and may eventually provide clues about how the clock is linked to output paths that yield observable rhythmic behaviors.

REFERENCES AND NOTES

1. R. J. Konopka and S. Benzer, *Proc. Natl. Acad. Sci. U.S.A.* **68**, 2112 (1971).
2. M. K. Baylies, T. A. Bargiello, F. R. Jackson, M. W. Young, *Nature* **326**, 390 (1987); Q. Yu *et al.*, *Proc. Natl. Acad. Sci. U.S.A.* **84**, 784 (1987).
3. P. E. Hardin, J. C. Hall, M. Rosbash, *Nature* **343**, 536 (1990); *EMBO J.* **11**, 1 (1992); *Proc. Natl. Acad. Sci. U.S.A.* **89**, 11711 (1992); P. E. Hardin, *Mol. Cell. Biol.* **14**, 7211 (1994).
4. A. Sehgal, J. L. Price, B. Man, M. W. Young, *Science* **263**, 1603 (1994).
5. K. K. Siwicki, C. Eastman, G. Petersen, M. Rosbash, J. C. Hall, *Neuron* **1**, 141 (1988).
6. D. M. Zerr, J. C. Hall, M. Rosbash, K. K. Siwicki, *J. Neurosci.* **10**, 2749 (1990).
7. X. Liu *et al.*, *J. Neurosci.* **12**, 2735 (1992); L. Saez and M. W. Young, *Mol. Cell. Biol.* **8**, 5378 (1988).
8. I. Edery, L. J. Zwiebel, M. E. Dembinska, M. Rosbash, *Proc. Natl. Acad. Sci. U.S.A.* **91**, 2260 (1994).
9. L. B. Vosshall, J. L. Price, A. Sehgal, L. Saez, M. W. Young, *Science* **263**, 1606 (1994).
10. H. Zeng, P. E. Hardin, M. Rosbash, *EMBO J.* **13**, 3590 (1994).
11. F. R. Jackson, T. A. Bargiello, S. H. Yun, M. W. Young, *Nature* **320**, 185 (1986); Y. Citri *et al.*, *ibid.* **326**, 42 (1987).
12. S. T. Crews, J. B. Thomas, C. S. Goodman, *Cell* **52**, 143 (1988); E. C. Hoffman *et al.*, *Science* **252**, 954 (1991); K. M. Burbach, A. Poland, C. A. Bradfield, *Proc. Natl. Acad. Sci. U.S.A.* **89**, 8185 (1992).
13. H. Reyes, S. Reisz-Porszasz, O. Hankinson, *Science* **256**, 1193 (1992).
14. Z. J. Huang, I. Edery, M. Rosbash, *Nature* **364**, 259 (1993).
15. Z. J. Huang, K. D. Curtin, M. Rosbash, *Science* **267**, 1169 (1995).
16. N. Matsushita, K. Sogawa, M. Ema, A. Yoshida, Y. Fujii-Kuriyama, *J. Biol. Chem.* **268**, 21002 (1993); M. L. Whitelaw, J. A. Gustafsson, L. Poellinger, *Mol. Cell. Biol.* **14**, 8343 (1994).
17. J. L. Price, M. E. Dembinska, M. W. Young, M. Rosbash, *EMBO J.* **14**, 4044 (1995).
18. J. J. Sekelsky *et al.*, *Genetics* **139**, 1347 (1995).
19. A. Rothenfluh-Hilfiker and M. W. Young, unpublished data.
20. S. Cohen, personal communication.
21. Z. Shubo *et al.*, *EMBO J.* **14**, 2884 (1995).
22. C. S. Wesley, M. P. Myers, M. W. Young, *Nucleic Acids Res.* **22**, 538 (1994).
23. V. Pirrotta, in Drosophila: *A Practical Approach*, D. B. Roberts, Ed. (IRL, Oxford, 1986), pp. 83–110.
24. M. P. Myers, unpublished data.
25. S. Kidd, T. J. Lockett, M. W. Young, *Cell* **34**, 421 (1983); M. R. Kelley, S. Kidd, W. A. Deutsch, M. W. Young, *ibid.* **51**, 539 (1987).
26. A. Sehgal *et al.*, *Science* **270**, 808 (1995).
27. N. Gekakis *et al.*, *ibid.*, p. 811.
28. B. A. Hamilton, M. J. Palazzolo, E. M. Meyerowitz, *Nucleic Acids Res.* **19**, 1951 (1991).
29. R. E. Breitbart, A. Andreadis, B. Nadal-Ginard, *Annu. Rev. Biochem.* **56**, 467 (1987).
30. M. P. Myers, K. Wager-Smith, M. W. Young, data not shown.
31. K. Sogawa *et al.*, *Proc. Natl. Acad. Sci. U.S.A.* **92**, 1936 (1995).

32. We thank J. Lucchesi for providing the P1 clone 117 and W. Gelbart for providing *Df(2L)DTD62* 2^{P} 3^{D}; *H7* 3^{P} 2^{D}. P1 clone DSO2465 and *Drosophila* stocks 101-1, P1481, 145-7 and 145-12 were obtained from the Berkeley *Drosophila* Genome Project. We thank K. Matthews, Bloomington *Drosophila* Stock Center, for assistance with strains, and those maintaining FlyBase and the members of the Berkeley *Drosophila* Genome Project for organization and public distribution of mapped genomic clones and P-element insertion stocks. We thank G. Blobel, J. Friedman, M. Rosbash, J. Rutila, H. Zeng, and N. D. Zinder for discussions and comments on the manuscript. Supported by Howard Hughes Medical Institute (M.P.M., K.W.-S., C.S.W., M.W.Y.), the NSF Science and Technology Center for Biological Timing (M.W.Y. and A.S. for work performed at Rockefeller University), NSF (A.S. for work performed at the University of Pennsylvania), the Research Foundation at the University of Pennsylvania (A.S.), and an American Cancer Society Junior Faculty Research Award (A.S.). M.W.Y. is an Investigator in the Howard Hughes Medical Institute.

31 July 1995; accepted 3 October 1995

Rhythmic Expression of *timeless*: A Basis for Promoting Circadian Cycles in *period* Gene Autoregulation

Amita Sehgal,* Adrian Rothenfluh-Hilfiker, Melissa Hunter-Ensor, Yifeng Chen, Michael P. Myers, Michael W. Young

The clock gene *timeless* (*tim*) is required for circadian rhythmicity in *Drosophila*. The accumulation of *tim* RNA followed a circadian rhythm, and the phase and period of the *tim* RNA rhythm were indistinguishable from those that have been reported for *per*. The *tim* RNA oscillations were found to be dependent on the presence of PER and TIM proteins, which demonstrates feedback control of *tim* by a mechanism previously shown to regulate *per* expression. The cyclic expression of *tim* appears to dictate the timing of PER protein accumulation and nuclear localization, suggesting that *tim* promotes circadian rhythms of *per* and *tim* transcription by restricting *per* RNA and PER protein accumulation to separate times of day.

The *tim* gene, which we recently cloned (*1*), is essential for the production of circadian rhythms in *Drosophila* (*2*, *3*). Molecular data indicated that TIM protein may be required at a specific time of day to allow accumulation and nuclear localization of the PER protein (*2*–*4*), so we determined if expression of the *tim* gene showed temporal regulation. We examined the expression in heads of adult *Drosophila* for the following reasons: (i) The clock is known to be located in the head (*5*). (ii) Oscillation of *per* RNA was first demonstrated in adult heads, although subsequently it was shown to occur in most body tissues as well (*6*, *7*). (iii) All effects of *tim* on *per* RNA and PER protein have been studied in adult heads (*2*–*4*).

Adult flies were maintained in the presence of 12-hour light: 12-hour dark cycles (LD 12:12), and the amount of *tim* RNA in the heads was measured at 4-hour intervals over 4 days (Fig. 1). We found that *tim* RNA quantities oscillated during the course of LD12:12, with peak quantities corresponding to the end of the day and lowest quantities to dawn. Oscillations of *per* RNA have the same phase (*2*, *6*, *7*). The amplitude of the variation in *tim* RNA quantities appeared similar to that reported for *per* (*2*, *6*). On some days there was as much as a 15-fold difference between peak and trough amounts (Fig. 1B, day 1).

Oscillations of *per* RNA persist in constant darkness and are, therefore, considered a circadian rhythm (*6*), and oscillations of the RNA encoded by the *frequency* (*frq*) clock gene in *Neurospora* also persist in the absence of environmental signals (*8*). We studied the expression of *tim* and *per* RNA in wild-type and per^{S} (short-period mutant) flies under free-running conditions and found that oscillations of both *per* and *tim* RNA persist in constant darkness with indistinguishable periods, phases, and amplitudes (Fig. 2). The plot of *tim* RNA oscillations is essentially superimposed on the curve displaying *per* RNA cycling. Whereas both RNAs cycle with a ~23-hour periodicity in the wild type, they cycle in per^{S} with a 17- to 18-hour period (Fig. 2). The amplitude of the oscillations in wild-type and per^{S} flies is, however, reduced in

A. Sehgal, M. Hunter-Ensor, Y. Chen, Department of Neuroscience and Center for Sleep and Respiratory Neurobiology, University of Pennsylvania Medical Center, Philadelphia, PA 19104, USA.

A. Rothenfluh-Hilfiker, M. P. Myers, M. W. Young, Howard Hughes Medical Institute, National Science Foundation Science and Technology Center for Biological Timing, and the Laboratory of Genetics, Rockefeller University, New York, NY 10021, USA.

*To whom correspondence should be addressed.